

This document is the Accepted Manuscript version of a Published Work that appeared in final form in **MACROMOLECULES**, copyright © American Chemical Society after peer review and technical editing by the publisher. To access the final edited and published work see <https://pubs.acs.org/doi/10.1021/acs.macromol.0c02307>

Postprint of: Jasińska-Walc L., Duchateau R., Bouyahyi M., Aarts J., Syed A., Delsman E., How Chain Transfer Leads to a Uniform Polymer Particle Morphology and Prevents Reactor Fouling, *MACROMOLECULES* (2021), DOI: [10.1021/acs.macromol.0c02307](https://doi.org/10.1021/acs.macromol.0c02307)

# How Chain Transfer Leads to Uniform Polymer Particle Morphology and Prevents Reactor Fouling.

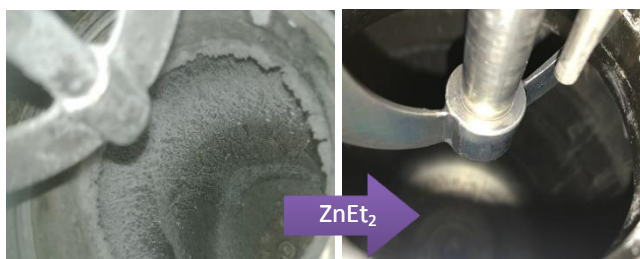
*Joey Aarts,<sup>a</sup> Amin Syed,<sup>a</sup> Miloud Bouyahyi,<sup>a</sup> Lidia Jasinska-Walc,<sup>a,b</sup>*

*Erik Delsman,<sup>a</sup> Rob Duchateau<sup>\*a,c</sup>*

<sup>a</sup> SABIC Technology & Innovation, STC Geleen, Urmonderbaan 22, Geleen, the Netherlands.

<sup>b</sup> Department of Polymer Technology, Chemical Faculty, Gdansk University of Technology, G. Narutowicza Str. 11/12, 80-233 Gdansk, Poland.

<sup>c</sup> Engineering and Technology Institute Groningen, University of Groningen, Nijenborgh 4, 9747 AG Groningen, The Netherlands.



**KEYWORDS:** polyolefin, homogeneous catalyst, chain transfer, morphology control, reactor fouling

**ABSTRACT:** The effect of adding diethyl zinc as chain transfer agent during the polymerization of propylene in heptane performed at 80 °C was studied. Although it was expected that chain transfer would stop after precipitation of the polymer, the polymer molecular weight continued to increase throughout the whole duration of the polymerization. The presence of diethyl zinc had the additional effect that the polymerizations were devoid of reactor fouling. To unravel this phenomenon, the polymer particle morphology was studied. Under the conditions applied, surprisingly uniform platelet-shaped polymer particles were formed. At high polymer content, these particles aggregate into microfibrillar structures consisting of nematic columnar strands of the same uniform platelets. The polymer particle morphology, as a result of controlled crystallization, is believed to play a crucial role in preventing reactor fouling.

## INTRODUCTION

Single-site olefin polymerization catalysts (SSC's) gradually found increasing application in the manufacturing of new types of polyolefins, either in their homogeneous nature in solution processes or as supported catalysts in slurry or gas phase processes.<sup>1</sup> During solution polymerization, the polymer product remains dissolved in the solvent, which means that for semi-crystalline polymers the polymerization has to be performed at least above the cloud point temperature to avoid precipitation and reactor fouling. Both gas phase and slurry polymerizations are performed well below the melting point of the polymer as they rely on the formation of solid polymer particles during the polymerization process. For the latter two processes, reactor fouling and polymer particle morphology are very important issues. Hence, heterogeneous catalysts—Ziegler-Natta, Phillips-type catalysts or supported SSC's—are used in these processes that produce morphologically uniform polymer particles of the appropriate size and shape as a result

of the replication phenomenon.<sup>1-3</sup> Reactor fouling can still be an issue, but this is mainly due to electrostatics, the formation of hot spots or deposition of waxes or partly hydrolyzed aluminum alkyls on the reactor wall.<sup>4</sup>

Initial research efforts directed towards the development of new SSC's are generally performed using unsupported catalysts at relatively low temperature, conditions that are very different from any of the industrially applied conditions: either slurry or gas phase using supported SSC's or high temperature solution phase using unsupported SSC's. During such low temperature lab-scale experiments the polymerization starts homogeneously but gradually more and more of the semi-crystalline polymer precipitates from solution, typically forming highly irregular polymer particles, chunks, sheets and fines. This precipitation is often accompanied with severe reactor fouling due to crystallization of the polymer on the reactor interior, which causes inhomogeneous heat transfer and monomer diffusion; no optimal conditions to evaluate and compare catalysts' performances.

The ability to study SSC's during low temperature lab-scale experiments free from issues like reactor fouling, poor morphology control or heat/mass transfer issues, would provide better insight in their true catalytic performance. Hence, finding a way to control the polymer particle growth of homogeneous catalysts while avoiding reactor fouling would be highly desired.

Several reports have appeared describing the control over polymer crystallization using homogeneous catalysts at low temperature. Mecking and coworkers<sup>5</sup> produced stable aqueous dispersions of polyethylene by micro-emulsion polymerizing of ethylene using palladium catalysts. Ronca et al.<sup>6</sup> prevented aggregation and uncontrolled precipitation of nascent ultra-high molecular weight polyethylene by polymerizing ethylene in the presence of dissolved LLDPE using a titanium phenoxyimine catalyst. Alt and coworkers<sup>7</sup> developed the so-called



self-immobilization technology, which afforded good morphology control without reactor fouling by the enchainment of the homogeneous catalyst in the produced polymer. Although remarkable results have been obtained, these methods are limited to certain polymers and/or catalyst types, which limits their versatility.

As part of a study on the efficiency of diethyl zinc (DEZ) as a reversible chain transfer agent for various SSC's during olefin polymerization, we accidentally discovered that ethylene and propylene polymerizations performed well below the polymer melting point (80 °C) using metallocene catalysts in the presence of DEZ were devoid of any reactor fouling, whereas severe reactor fouling was observed in the absence of DEZ (Figure S1). Furthermore, isotactic polypropylene produced in the presence of DEZ was recovered as a fine free-flowing powder without chunks, sheets, fibers and fines as usually obtained. This behavior was also noticed during ethylene polymerization and is not limited to a specific SSC. As it seemed to be a general and very useful feature, we decided to look into it deeper for propylene polymerization.

## RESULTS AND DISCUSSION

The importance of the presence of DEZ in preventing reactor fouling and yielding a uniform polymer powder morphology encouraged us to further study the chain transfer to zinc during propylene polymerization and its effect on polymer particle morphology and reactor fouling. It was argued that the presence of DEZ during a polymerization would initially result in a pseudo-living Coordinative Chain Transfer Polymerization (CCTP) system where the number of simultaneously growing chains would be proportional to the DEZ concentration whilst the propagation rate of the individual growing chains would be inversely proportional to the DEZ concentration.<sup>8-16</sup> Depending on the DEZ concentration and the kinetics of chain propagation and

chain transfer, tuning the  $k_{\text{propagation}}/k_{\text{crystallization}}$  ratio to lower values for such a CCTP system might allow the polymer to crystallize in a controlled manner from solution. Subsequently, the thus formed polymer particles—the surface of which exceeds the surface of the reactor wall by several orders of magnitude—might function as seeds for newly formed polymer chains, produced under non-CCTP conditions, thereby avoiding reactor fouling and providing good morphology control.<sup>7,17,18</sup>

**Table 1.** Details of polymerization reactions using varying TiBA and MAO concentrations.<sup>a</sup>

Entry #	MAO mM	TiBA mM	Yield <sup>b</sup> g	Activity 10 <sup>6</sup> pol/(mol·h)	$M_n$ g	$M_n$ kg·mol <sup>-1</sup>	$\bar{D}$	$T_m$ °C
1	6.0	1.47	105	656	29.5	62.0	2.1	153
2	0.6	0.15	9	56	23.1	64.7	2.8	152
3	0.6	1.47	11	69	43.0	103.2	2.4	152
4	6.0	0.15	126	788	27.4	63.0	2.3	153
5	3.0	0.15	122	763	27.2	62.6	2.3	151
6	1.5	0.15	56	350	28.2	59.2	2.1	152

a) Conditions: reaction performed in a stirred 2 L stainless-steel fed-batch reactor (Büchi); heptane: 1.5 L; stirring speed: 300 RPM; temperature: 80 °C; propylene pressure: 5 bar; catalyst: *rac*-Me<sub>2</sub>Si(2-Me-4-Ph-Ind)<sub>2</sub>ZrCl<sub>2</sub>: 0.21 μM; DEZ (1.5 M in toluene): 1.0 mM; reaction time: 30 minutes. b) Yield was obtained after drying the polymer overnight under reduced pressure at 80 °C in a vacuum oven.

In an attempt to approach industrial slurry polymerization process conditions, the polymerization studies were performed in heptane at 80 °C. For this study we limited ourselves to the homogeneous MAO-activated *rac*-Me<sub>2</sub>Si(2-Me-4-Ph-Ind)<sub>2</sub>ZrCl<sub>2</sub> as the catalyst. In order to reliably study polymerization processes, the polymerizations should run under

conditions that are not mass transfer limited. For the reactor setup used, a stirring speed of 300 RPM was found to be sufficient as long as the catalyst concentration was kept low ( $\leq 0.25 \mu\text{M}$ , see Supporting Information, Figures S2, S3). Different amounts of MAO as cocatalyst and TiBA as scavenger were applied to evaluate possible effects on catalytic activity as well as polymer molecular weight and melting temperature (Table 1). The fact that increasing the scavenger concentration by one order of magnitude had little effect on the activity while increasing the MAO concentration had a significant effect suggests that incomplete catalyst activation rather than catalyst poisoning by impurities is responsible for the low activity observed at low MAO concentrations.<sup>19</sup> Increasing the MAO concentration to 3.0 mM afforded good activity, while further increase in MAO concentration did not lead to a significant further increase in activity. The lower activity at high TiBA concentrations might indicate partial catalyst deactivation by the formation of dormant hetero-bimetallic zirconium-aluminum ato species.<sup>9,10,20</sup> Control experiments (Table S1) revealed that adding BHT<sup>21</sup> did not result in a significant increase of the molecular weight, suggesting that chain transfer to aluminum is negligible for this catalyst system.<sup>9,22</sup>

**Effect of the presence of DEZ on the activity and polymer molecular weight.** To study the effect of DEZ on the catalytic activity, the polymer molecular weight and the polydispersity, polymerization reactions using three different DEZ concentrations have been performed (Table 2, entries 1 – 4). Increasing the DEZ concentration resulted in a significant drop of the molecular weight, proving that DEZ is an effective CTA for the applied zirconocene catalyst (Figure 1). The catalytic activity showed a linear decrease with increasing DEZ concentration (Figure 2A). This first order dependency is in agreement with the possible formation of inactive hetero-bimetallic zirconium-zinc complexes that form the intermediates of the chain transfer

process.<sup>9,10,17</sup> Another direct proof that DEZ functions as a CTA was provided by the experiment in which first the catalyst was dosed and was allowed to start polymerizing before DEZ was added. Sampling over time clearly showed that initial high molecular weight polypropylene was formed. Once DEZ was added the molecular weight dropped considerably after which it gradually increased with polymerization time (Figure S4). Next, polymerization reactions were performed using two different catalyst concentrations while keeping the DEZ concentration the same. Comparing entries 3 with 6, 4 with 7 and 8 with 9 of Table 2, respectively, it is clear that increasing the catalyst concentration from 0.21 to 0.42  $\mu\text{M}$  in the presence of TiBA resulted in a lower than expected activity, which is likely the result of mass transfer limitation. When more DEZ (Table 2, entries 4, 7) was added, which lowers the activity, or no TiBA scavenger was used (Table 2, entries 8, 9), then the yield was roughly proportional to the catalyst concentration. The molecular weight of the products obtained using the same DEZ concentration in the absence of TiBA were slightly lower than with TiBA. TiBA is known to react with DEZ producing inactive metallic zinc.<sup>23</sup> In principle this side reaction could result in a lower effective DEZ concentration, which consequently would result in a higher molecular weight of the polymer obtained. However, except experiment 2 from Table 2, all experiments were performed with a significantly higher DEZ than TiBA concentration so only a limited amount of DEZ might be sacrificed by this process. This is supported by the significant difference in molecular weight for entries 2 and 3 and the small difference in molecular weight between entries 3 and 8. Doubling of the catalyst concentration while keeping the DEZ concentration constant has, as expected, no effect on the molecular weight (Figure 3).

**Table 2.** Propylene polymerization in heptane using varying catalyst, DEZ and TiBA concentrations.<sup>a</sup>

Entry #	Cat. $\mu\text{M}$	DEZ mM	TiBA mM	Yield <sup>b</sup> g	Activity $10^6 \text{ g pol}/(\text{mol}\cdot\text{h})$	$M_n$ $\text{kg}\cdot\text{mol}^{-1}$	$M_w$ $\text{kg}\cdot\text{mol}^{-1}$	$\bar{D}$	mmol chains/ #chains:Zn/ #chains:Zr	$T_m$ $^\circ\text{C}$
1	0.21	0	0.20	169	1,065 <sup>c</sup>	81.0	186.3	2.3	2.1/0/6,600	153
2	0.21	0.2	0.15	190	792	51.0	112.2	2.2	3.7/12.4/11,800	153
3	0.21	1.0	0.15	152	633	33.3	73.3	2.2	4.6/4.6/14,500	152
4	0.21	2.0	0.15	70	292	15.4	38.5	2.5	4.5/2.3/14,400	155
5	0.21	1.0	0.15	247	444 <sup>d</sup>	34.1	81.8	2.4	7.2/7.2/23,000	152
6	0.42	1.0	0.15	183	381	31.2	71.8	2.3	5.9/5.9/9,300	153
7	0.42	2.0	0.15	179	373	21.4	53.5	2.5	8.4/4.2/13,300	152
8	0.21	1.0	0	95	396	27.2	59.8	2.2	3.5/3.5/11,100	153
9	0.42	1.0	0	170	354	29.6	68.1	2.3	5.7/5.7/9,100	152
10	0.21	1.0	2	12	75	38.8	85.4	2.2	0.3/0.2/1,000	153
11	0.21	2.0	0.2	148	310	20.5	53.3	2.6	7.2/3.6/22,900	152

a) Conditions: reaction performed in a stirred 2 L stainless-steel fed-batch reactor (Büchi). Heptane: 1.5 L; stirring speed: 300 RPM; temperature: 80 °C; propylene pressure: 5 bar; MAO: 3.0 mM; catalyst: *rac*-Me<sub>2</sub>Si(2-Me-4-Ph-Ind)<sub>2</sub>ZrCl<sub>2</sub>; polymerization time: 45 min. b) Yield was obtained after drying the polymer overnight under reduced pressure at 80 °C in a vacuum oven. c) Polymerization time: 30 min. d) Polymerization time: 100 min.





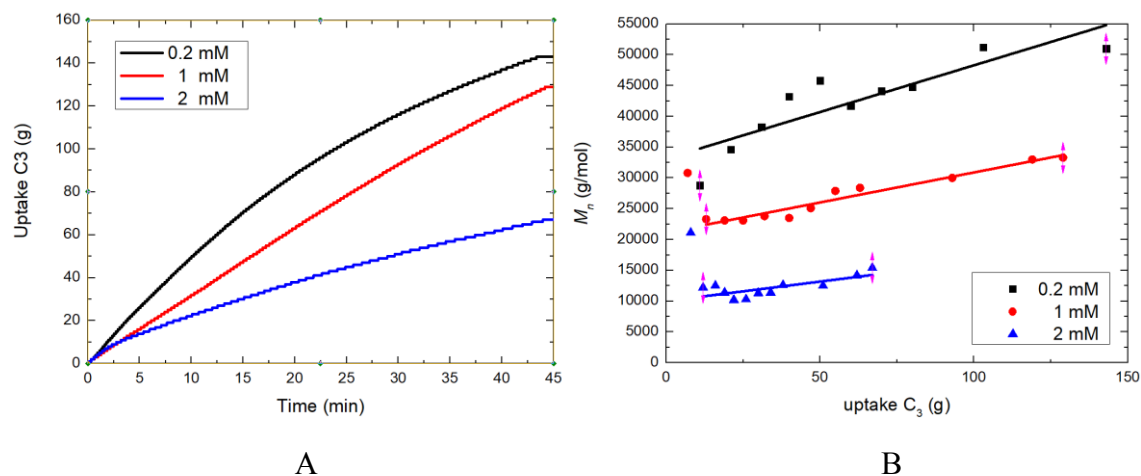


**Figure 1.** (A) Propylene uptake profile and (B) development of  $M_n$  versus propylene ( $C_3$ ) uptake, for different DEZ concentrations at a fixed catalyst concentration (Table 2, entries 2–4).

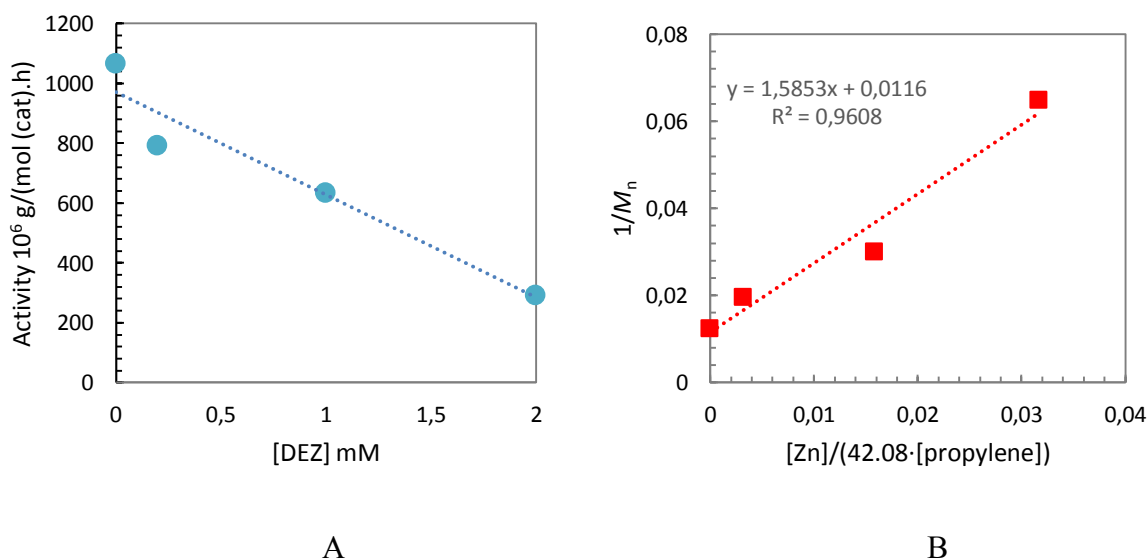


**Figure 2.** (A) Dependence of catalytic activity on DEZ concentration and (B) Mayo plot of  $1/M_n$  versus  $[\text{Zn}]/(42.08 \cdot [\text{propylene}])$ , (Table 2, entries 1 – 4).

Although it is clear that chain transfer to zinc takes place, the fact that the molecular weights do not increase proportional with the propylene consumption (Figure 1B) and that the

polydispersity indices are  $> 2$  indicate that the system is clearly not running under reversible, living CCTP conditions.<sup>12-16,24</sup> Although this value should be treated with caution for a system in which the polymer containing the CTA precipitates,<sup>25</sup> the  $k_{ct}:k_{cg}$  of 1.6 obtained from the Mayo plot (Figure 2B)<sup>26</sup> clearly demonstrates that the rate constants for chain transfer ( $k_{ct}$ ) and chain growth ( $k_{cg}$ ) are of the same order of magnitude.<sup>27-29</sup> This means that under the polymerization conditions applied the actual rate of chain transfer is relatively low compared to the rate of polymerization. <sup>1</sup>H NMR analysis on the polymers qualitatively showed the existence of vinylidene and vinyl end groups indicating that competitive  $\beta$ -H and  $\beta$ -Me transfer is taking place as well (Figure S5). This is in agreement with the observation that the number of polymer chains formed exceeds the amount of zinc present in the system (Table 2).

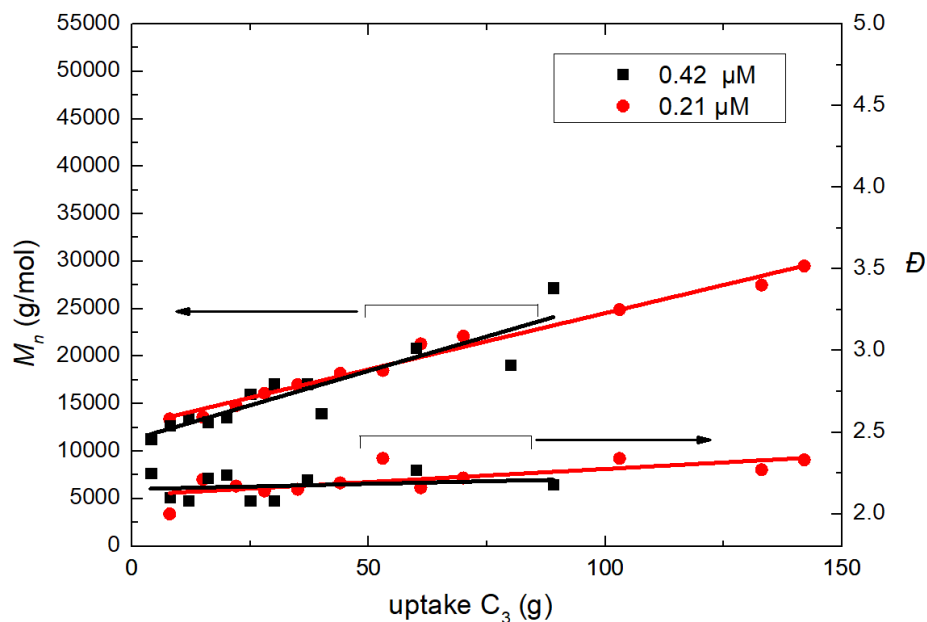


**Figure 3.**  $M_n$  development versus propylene ( $C_3$ ) uptake for two different catalyst concentrations and evolution of the polydispersity ( $D$ ) versus propylene uptake for two different catalyst concentrations (Table 2, entries 8, 9).

Interestingly, for the experiments displayed in Figure 1B and 3, the number average molecular weight increases linearly with time during the whole polymerization period. Whereas this might seem to suggest that reversible chain transfer proceeds until the end of the polymerization despite the fact that polymer precipitated under the polymerization process conditions applied, this is not necessarily the case. It is generally accepted that precipitation of the CTA-containing polymer—separated from solution once the polymer chains have reached a critical molecular weight—leads to heterogenization of the system combined with a strong decrease in chain transfer rate and consequently a rather broad polydispersity.<sup>30,31</sup> As the chain transfer to zinc is relatively slow, the zinc-polymeryls precipitate only gradually from the solution during the polymerization process. Consequently, the zinc alkyl concentration in solution also progressively drops leading to increasing molecular weights with polymerization time and a broadening of the polydispersity.

Summarizing, both the catalytic activity and the molecular weight of the produced polymers show a near linear dependence on the DEZ concentration indicating that DEZ is an effective CTA, albeit that under the applied conditions the chain transfer appears to be rather slow and probably irreversible. Both the relatively slow (and likely irreversible) chain transfer to zinc and the concurrent  $\beta$ -H and  $\beta$ -Me transfer are in agreement with the relatively broad polydispersity and gradual but non-proportional increase of the polymer molecular weight with polymerization time. If chain transfer would be fast under these conditions, a bimodal molecular weight distribution as would be expected similar as was observed for irreversible chain transfer to zinc under solution polymerization conditions.<sup>25,27</sup>

**Polymer powder morphology and reactor fouling.** The most obvious reason why the addition of DEZ prevented reactor fouling would be the formation of lower molecular weight products. Low molecular weight products dissolve better, which gives them more time to gradually crystallize from solution. However, with number average molecular weights of up to  $50 \text{ kg}\cdot\text{mol}^{-1}$  obtained in this study (Tables 2), this is unlikely to be the main reason behind preventing reactor fouling. To get insight into the solubility of the polymers, cloud point tests were performed. As expected, the solubility of the polymers is inversely proportional to the molecular weight of the polymers (Figure S6). For the polymerization conditions applied, polypropylene samples with number average molecular weights typically below  $80 \text{ kg}\cdot\text{mol}^{-1}$  were obtained. For these polymers, at  $80 \text{ }^\circ\text{C}$  in heptane the cloud points lie around 3 – 4 wt%. With a typical solid content at the end of the polymerization reaction in the presence of diethyl zinc of 10 – 20 wt%, this seems limited, but during the initial stage of the polymerization reaction a notable fraction of the polymer is dissolved. Control experiments carried out in the absence of diethyl zinc (e.g. Table 2, entry 1; Table S1, entries 1 and 2) were encumbered by severe reactor fouling, already at moderate polymer content (5 – 10 wt%), resulting in laborious cleaning of the reactor.

**Polymer morphology and reactor fouling.** To better understand what might be the reason for the lack of reactor fouling in the presence of diethyl zinc, the morphologies of polymer samples having different molecular weight collected from the reactor at different solid content were analyzed. All samples were treated equally: after being discharged from the reactor, the product mixtures were cooled to approx.  $40 \text{ }^\circ\text{C}$ , treated with acidified isopropanol, filtered and dried in a vacuum oven at  $80 \text{ }^\circ\text{C}$ . Figure 4 shows SEM pictures of isotactic polypropylene samples with similar molecular weights ( $M_n \sim 35 \text{ kg}\cdot\text{mol}^{-1}$ ) collected at different solid content (1, 12 and



18 wt%, respectively) in the reactor. As can be seen, the morphologies of the samples are dramatically different. For the sample with the lowest solid content (1 wt%) spherical porous particles were observed, whilst at 12 wt% the product displays a platelet-like morphology. It is worth mentioning that these platelets are surprisingly uniform in both size and shape. Finally, at a high polymer content of 18 wt%, microfibrillar structures are obtained (Figure 4C). Upon a closer look, these microfibrils appeared to consist of nematic columnar<sup>32,33</sup> strands of the small platelets found for the medium polymer content in the reactor (Figure 4B and 4C). The formation of these microfibrils is likely the result of the anisotropy and high uniform size and shape of the principle particles.

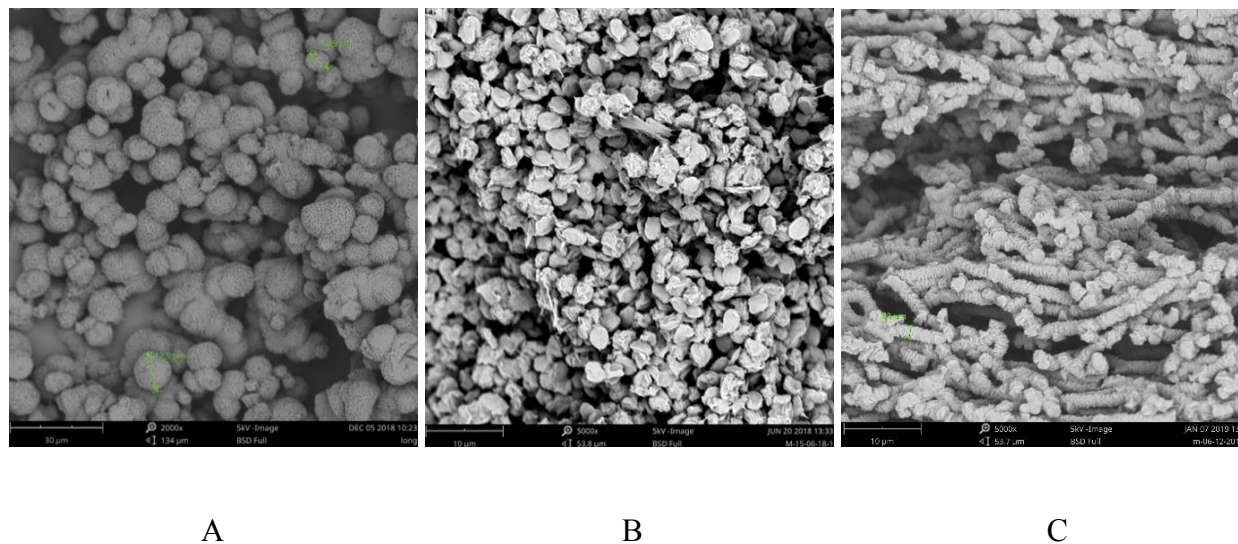


**Figure 4.** SEM images of isotactic polypropylenes with constant  $M_n$  of  $35 \text{ kg}\cdot\text{mol}^{-1}$  produced with increasing wt% inside the reactor: (A) 1 wt% (Table 2, entry 10), (B) 12 wt% (Table 2, entry 3), (C) 18 wt% (Table 2, entry 5).

Interestingly, very similar morphologies were observed for polypropylene samples of different molecular weights collected at the same polymer content of  $13 \pm 1.5$  wt% in the reactor (Figure S7). Whereas the lowest molecular weight sample consist of spherical, porous structures, the medium molecular weight product displays a uniform platelet-like morphology and the high molecular weight sample shows microfibrillar structures consisting of stacked platelets. Hence, there seems to be a correlation between the polymer molecular weight and the solid content determining the morphology of the polymer.

Based on cloud point temperature measurements, the polypropylene with a molecular weight of  $35 \text{ kg}\cdot\text{mol}^{-1}$  should be fully dissolved in heptane at a 1 wt% solid content at  $80 \text{ }^\circ\text{C}$ . Therefore, it seems that this spherical porous morphology is formed when the polymer crystallizes upon cooling of the product mixture after the polymerization is completed. At 12 wt% solid content, the majority of the polypropylene with a molecular weight of  $35 \text{ kg}\cdot\text{mol}^{-1}$  is insoluble at  $80 \text{ }^\circ\text{C}$ , which means that these platelets (Figure 4B) have been formed by crystallization during the polymerization process. However, throughout the whole polymerization process around 3 wt% (this corresponds to approx. 30 g) of polymer with an  $M_n$  of  $35 \text{ kg}\cdot\text{mol}^{-1}$  remains soluble at  $80 \text{ }^\circ\text{C}$ . This relatively high fraction of soluble polymer (including zinc polymeryls) might also explain the unexpected gradual increase in molecular weight during the whole duration of the polymerization process (Figures 1B, 3) as chain transfer can continue for the soluble fraction of zinc polymeryls. Keeping in mind that the molecular weight of the polymer increases with polymerization time, at the beginning of the polymerization the fraction of soluble polymer has been even higher. The high uniformity of the platelets suggests that possibly they are formed in polymer-rich droplets of the same size that could be formed after liquid-liquid phase separation.

The morphology is quite different compared to that obtained by thermal induced phase separation of saturated isotactic polypropylene solutions.<sup>34,35</sup>

Both polypropylene with a number average molecular weight of  $51 \text{ kg}\cdot\text{mol}^{-1}$  at a solid content of 14.5 wt% and polypropylene with a number average molecular weight of  $35 \text{ kg}\cdot\text{mol}^{-1}$  at 18 wt% solid content gave the same peculiar fibrillary structures consisting of strands of the uniform platelet particles. The combination of the anisotropy and high uniformity of the principle particles most likely give rise to the formation of these fibrils. Furthermore, during the crystallization process in the reactor (at  $80 \text{ }^\circ\text{C}$ ), there is likely to be a dynamic equilibrium of dissolved and crystallized polymer. Once this polymer crystallizes, it is expected that the crystal surface is somewhat “hairy” as a result of the partial solubility of the polypropylene in heptane (Figure 5). These brushes determine the so-called excluded volume of the crystallized polymer particles.<sup>36</sup> When the concentration of these crystals increases, the excluded volumes of the individual platelets start to overlap, which leads to entanglement and eventually crystallization of these brushes to form the nematic columnar structures.<sup>32,33</sup>

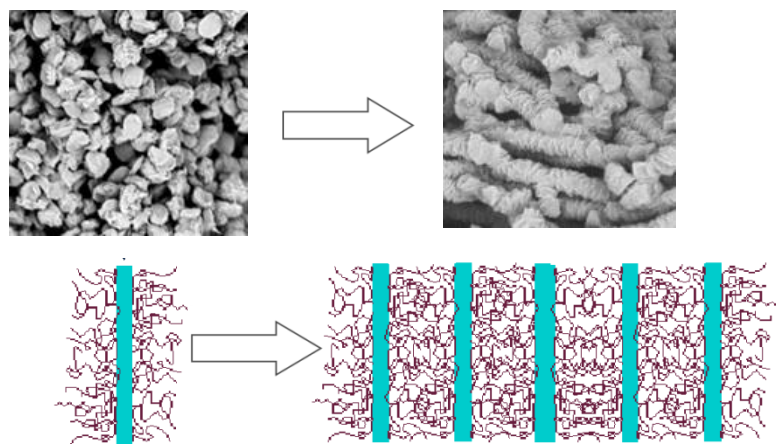


**Figure 5.** Self-assembly of platelets into nematic columnar microfibrillary structures.

When the polymer content—and with that the microfibrils concentration—becomes high (i.e. 18 wt% for entry 5 in Table 2) the product is retrieved from the reactor as a kind of gel that retains a lot of solvent (Figure S8). Although this results in some reactor fouling, the polymer product does not stick strongly to the reactor wall and can easily be wiped off or removed by a washing step. Nevertheless, to avoid inhomogeneity and mass transfer limitation, it is recommended to keep the polymer concentration below 15 wt%.

## CONCLUSIONS

The observation that the average molecular weight gradually increased throughout the whole polymerization process was rather unexpected. However, considering the relatively slow and probably irreversible chain transfer to zinc, it might well be that the zinc-polymeryls only gradually precipitate from the solution during the polymerization. The combination of this reversible but slow chain transfer to zinc and competitive chain termination by  $\beta$ -H and  $\beta$ -Me transfer leads to a gradual increase in both the number of polymer chains and their molecular weight with time, rather than a bimodal molecular weight distribution as would be expected for irreversible chain transfer to zinc during solution polymerization<sup>25,27</sup> or fast reversible chain transfer to zinc followed by rather sudden precipitation of the zinc-polymeryls when the polymerization is performed below the melting point of the polymer. It is likely that the observed gradual increase of molar mass leads to a more controlled crystallization process to polymer particles of a highly uniformity, which on its turn prevents reactor fouling.



## ASSOCIATED CONTENT

The Supporting Information is available free of charge at ...

Experimental procedures, additional graphs and SEM pictures of polymer samples (PDF)

## AUTHOR INFORMATION

### **Corresponding Author**

Rob Duchateau – *SABIC Technology & Innovation, STC Geleen, Urmonderbaan 22, Geleen, the Netherlands; Engineering and Technology Institute Groningen, University of Groningen, Nijenborgh 4, 9747 AG Groningen, The Netherlands.*

*Email: Rob.Duchateau@SABIC.com*

### **Authors**

Joey Aarts – *SABIC Technology & Innovation, STC Geleen, Urmonderbaan 22, Geleen, the Netherlands.*

Amin Syed – *SABIC Technology & Innovation, STC Geleen, Urmonderbaan 22, Geleen, the Netherlands.*

Miloud Bouyahyi – *SABIC Technology & Innovation, STC Geleen, Urmonderbaan 22, Geleen, the Netherlands.*

Lidia Jasinska-Walc – *SABIC Technology & Innovation, STC Geleen, Urmonderbaan 22, Geleen, the Netherlands, Department of Polymer Technology, Chemical Faculty, Gdansk University of Technology, G. Narutowicza Str. 11/12, 80-233 Gdansk, Poland.*

Erik Delsman – *SABIC Technology & Innovation, STC Geleen, Urmonderbaan 22, Geleen, the Netherlands.*

### **Funding Sources**

This research was financially supported by SABIC.

### **Notes**

The authors declare no competing financial interest.

### **ACKNOWLEDGMENT**

Financial support by SABIC for this work is gratefully acknowledged.

### **REFERENCES**

1. Polyolefin Reactor Engineering, Soares, J. B. P.; McKenna, T. F. L. (eds.) Wiley-VCH, 2012 and references cited therein.
2. Severn, J. R.; Chadwick, J. C.; Duchateau, R.; Friederichs, N. “Bound but Not Gagged” – Immobilizing Single Site  $\alpha$ -Olefin Polymerization Catalysts. *Chem. Rev.* **2005**, *105*, 4073–4147.

3. Multimodal Polymers with Supported Catalysts – Design and Production. Albonia, A. R.; Prades, F.; Jeremic, D. (eds.). Springer 2019 and references cited therein.
4. Cardoso, M. N.; Fish, A. G. Mechanism of Fouling in Slurry Polymerization Reactors of Olefins. *Ind. Eng. Chem. Res.* **2016**, *55*, 9426–9432.
5. Bauers, F. M.; Thomann, R.; Mecking, S. Submicron Polyethylene Particles from Catalytic Emulsion Polymerization. *J. Am. Chem. Soc.* **2003**, *125*, 8838–8840.
6. Ronca, S.; Forte, G.; Ailianou, A.; Kornfield, J. A.; Rastogi, S. Direct Route to Colloidal UHMWPE by Including LLDPE in Solution during Homogeneous Polymerization of Ethylene. *ACS Macro Lett.* **2012**, *1*, 1116–1120.
7. Alt, H. G. Self-immobilizing catalysts and cocatalysts for olefin polymerization. *Dalton Trans.* **2005**, 3271–3276 and references cited therein.
8. van Meurs, M.; Britovsek, G. J. P.; Gibson, V. C.; Chen, S. A. Polyethylene Chain Growth on Zinc Catalyzed by Olefin Polymerization Catalysts: A Comparative Investigation of Highly Active Catalyst Systems across the Transition Series. *J. Am. Chem. Soc.* **2005**, *127*, 9913–9923.
9. Bhriain, N. N.; Brintzinger, H.-H.; Ruchatz, D.; Fink, G. Polymeryl Exchange between ansa-Zirconocene Catalysts for Norbornene–Ethylene Copolymerization and Aluminum or Zinc Alkyls. *Macromolecules* **2005**, *38*, 2056–2063.
10. Arriola, D. J.; Carnahan, E. M.; Hustad, P. D.; Kuhlman, R. L.; Wenzel, T. T. Catalytic Production of Olefin Block Copolymers via Chain Shuttling Polymerization. *Science* **2006**, *312*, 714–719.



11. Zhang, C.; Niu, H.; Dong, J.-Y. A novel effect of bis(6-heptenyl)zinc on the molecular weight and rheologic performance of polypropylene produced by *rac*-Me<sub>2</sub>Si[2-Me-4-Ph-Ind]<sub>2</sub>ZrCl<sub>2</sub>/MAO. *Polym. Bull.* **2010**, *65*, 779–786.
12. Zhang, W.; Sita, L. R. Highly Efficient, Living Coordination Chain-Transfer Polymerization of Propene with ZnEt<sub>2</sub>: Practical Production of Ultrahigh to Very Low Molecular Weight Amorphous Atactic Polypropenes of Extremely Narrow Polydispersity. *J. Am. Chem. Soc.* **2008**, *130*, 442–443.
13. Zhang, W.; Sita, L. R. Living Coordinative Chain-Transfer Polymerization and Copolymerization of Ethene,  $\alpha$ -Olefins, and  $\alpha,\omega$ -Nonconjugated Dienes Using Dialkylzinc as “Surrogate” Chain-Growth Sites. *Macromolecules* **2008**, *41*, 7829–7833.
14. Descour, C.; Macko, T.; Cavallo, D.; Parkinson, M.; Hubner, G.; Spoelstra, A.; Villani, M.; Duchateau, R. Synthesis and Characterization of iPP-sPP Stereoblock Produced by a Binary Metallocene System. *J. Polym. Sci., Part A: Polym. Chem.* **2014**, *52*, 1422–1434.
15. Kempe, R. How to Polymerize Ethylene in a Highly Controlled Fashion? *Chem. Eur. J.* **2007**, *13*, 2764 – 2773.
16. Valnte, A.; Mortreux, A.; Visseaux, M.; Zinck, P. Coordinative Chain Transfer Polymerization. *Chem. Rev.* **2013**, *113*, 3836 – 3857.
17. Hong, S. C.; Teranishi, T.; Soga, K. Investigation on the polymer particle growth in ethylene polymerization with PS beads supported *rac*-Ph<sub>2</sub>Si(Ind)<sub>2</sub>ZrCl<sub>2</sub> catalyst. *Polymer* **1988**, *39*, 7153–7157.



18. Klapper, M.; Joe, D.; Nietzel, S.; Krumpfer, J. W.; Müllen, K. Olefin Polymerization with Supported Catalysts as an Exercise in Microtechnology. *Chem. Mater.* **2014**, *26*, 802–819.
19. Spaleck, W.; Küber, F.; Winter, A.; Rohrmann, J.; Bachmann, B.; Antberg, M.; Dolle, V.; Paulus, E. F. The Influence of Aromatic Substituents on the Polymerization Behavior of Bridged Zirconocene Catalysts. *Organometallics* **1994**, *13*, 954–963.
20. Bochmann, M. The Chemistry of Catalyst Activation: The Case of Group 4 Polymerization Catalysts. *Organometallics* **2010**, *29*, 4711–4740.
21. Busico, V.; Cipullo, R.; Cutillo, F.; Friederichs, N.; Ronca, S.; Wang, B. Improving the Performance of Methylalumoxane: A Facile and Efficient Method to Trap “Free” Trimethylaluminum. *J. Am. Chem. Soc.* **2003**, *125*, 12402–12403.
22. Lahelin, M.; Kokko, E.; Lehmus, P.; Pitkänen, P.; Löfgren, B.; Seppälä, J. Propylene Polymerization with *rac*-SiMe<sub>2</sub>(2-Me-4-PhInd)<sub>2</sub>ZrCl<sub>2</sub>/MAO: Polymer Characterization and Kinetic Models. *Macromol. Chem. Phys.* **2003**, *204*, 1323–1337.
23. Périn, S. G. M.; Severn, J. R.; Koning, C. E.; Chadwick, J. C. Unusual effect of Diethyl Zinc and Triisobutylaluminium in Ethylene/1-Hexene Copolymerisation using an MgCl<sub>2</sub>-Supported Ziegler-Natta Catalyst. *Macromol. Chem. Phys.* **2006**, *207*, 50–56.
24. Mueller, A. H. E.; Zhuang, R.; Yan, D.; Litvinenko, G. Kinetic Analysis of “Living” Polymerization Processes Exhibiting Slow Equilibria. 1. Degenerative Transfer (Direct Activity Exchange between Active and “Dormant” Species. Application to Group Transfer Polymerization). *Macromolecules* **1995**, *28*, 4326–4333.



25. Hue, R. J.; Cibuzar, M. P.; Tonks, I. A. Analysis of Polymeryl Chain Transfer Between Group 10 Metals and Main Group Alkyls during Ethylene Polymerization. *ACS Catal.* **2014**, *4*, 4223–4231.
26. Mayo, F. R. Chain Transfer in the Polymerization of Styrene: The Reaction of Solvents with Free Radicals<sup>1</sup>. *J. Am. Chem. Soc.* **1943**, *65*, 2324–2329.
27. Cuency, E. S.; Johnson, H. C.; Anding, B. J.; Landis, C. R. Mechanistic Studies of Hafnium-Pyridyl Amido-Catalyzed 1-Octene Polymerization and Chain Transfer Using Quench-Labeling Methods. *J. Am. Chem. Soc.* **2017**, *139*, 11903–11012.
28. Johnson, H. C.; Cuency, E. S.; Landis, C. R. Chain Transfer with Dialkyl Zinc During Hafnium-Pyridyl Amido-Catalyzed Polymerization of 1-Octene: Relative Rates, Reversibility, and Kinetic Models. *ACS Catal.* **2018**, *8*, 4178–4188.
29. Cuency, E. S.; Johnson, H. C.; Landis, C. R. Selective Quench-Labeling of the Hafnium-Pyridyl Amido-Catalyzed Polymerization of 1-Octene in the Presence of Trialkyl-Aluminum Chain-Transfer Reagents. *ACS Catal.* **2018**, *8*, 11605–11614.
30. Pelletier, J.-F.; Mortreux, A.; Olonde, X.; Bujadoux, K. Synthesis of New Dialkylmagnesium Compounds by Living Transfer Ethylene Oligo- and Polymerization with Lanthanocene Catalysts. *Angew. Chem. Int. Ed. Engl.* **1996**, *35*, 1854–1856.
31. Kretschmer, W. P.; Meetsma, A.; Hessen, B.; Schmalz, T.; Qayyum, S.; Kempe, R. Reversible Chain Transfer between Organoyttrium Cations and Aluminum: Synthesis of Aluminum-Terminated Polyethylene with Extremely Narrow Molecular-Weight Distribution. *Chem. Eur. J.* **2006**, *12*, 8969–8978.



32. Chandrasekhar, S.; Ranganath, G. S.; Discotic liquid crystals. *Reports Prog. Phys.* **1990**, *53*, 57–84.
33. Kumar, S. Self-organization of disc-like molecules: chemical aspects. *Chem. Soc. Rev.* **2006**, *35*, 83–109.
34. Lloyd, D. R.; Kinzer, K. E.; Tseng, H. S. Microporous membrane formation via thermally induced phase separation. I. Solid–liquid phase separation. *J. Membrane Sci.* **1990**, *52*, 239–261.
35. Lee, H. K.; Myerson, A. S.; Levon, K. Nonequilibrium Liquid–Liquid phase separation in crystallizable polymer solutions. *Macromolecules* **1992**, *25*, 4002–4010.
36. Lu C.; Mai, Y.-W. in *Physical Properties and Applications of Polymer Microcomposites*. Tjong, S. C.; Mai, Y.-W. (eds.) ScienceDirect. **2010**, pages 431-453.